

Mosaic: Unlocking Long-Context Inference for Diffusion LLMs via Global Memory Planning and Dynamic Peak Taming

Liang Zheng¹ Bowen Shi¹ Yitao Hu¹ Jiawei Zhang¹ Ruofan Li¹ Sheng Chen¹ Wenxin Li¹ Keqiu Li¹

Abstract

Diffusion-based large language models (dLLMs) have emerged as a promising paradigm, utilizing simultaneous denoising to enable global planning and iterative refinement. While these capabilities are particularly advantageous for long-context generation, deploying such models faces a prohibitive memory capacity barrier stemming from severe system inefficiencies. We identify that existing inference systems are ill-suited for this paradigm: unlike autoregressive models constrained by the cumulative KV-cache, dLLMs are bottlenecked by *transient activations* recomputed at every step. Furthermore, general-purpose memory reuse mechanisms lack the global visibility to adapt to dLLMs' *dynamic memory peaks*, which toggle between logits and FFNs. To address these mismatches, we propose Mosaic, a memory-efficient inference system that shifts from local, static management to a global, dynamic paradigm. Mosaic integrates a mask-only logits kernel to eliminate redundancy, a lazy chunking optimizer driven by an online heuristic search to adaptively mitigate dynamic peaks, and a global memory manager to resolve fragmentation via virtual addressing. Extensive evaluations demonstrate that Mosaic achieves an average $2.71 \times$ reduction in the memory peak-to-average ratio and increases the maximum inference sequence length supportable on identical hardware by $15.89\text{-}32.98 \times$. This scalability is achieved without compromising accuracy and speed, and in fact reducing latency by 4.12%–23.26%.

1. Introduction

Autoregressive (AR) models have driven recent breakthroughs in generative AI (Zhao et al., 2023; Minaee et al., 2024). However, a new paradigm known as diffusion-based

¹Tianjin University, China. Correspondence to: Yitao Hu <yitao@tju.edu.cn>.

Preprint. January 13, 2026.

large language models (dLLMs) has emerged. Distinct from the sequential, left-to-right generation of AR, it progressively denoises the entire sequence simultaneously (Nie et al., 2025; Zhu et al., 2025; Ye et al., 2025). This capability enables global planning and iterative refinement, making it a promising paradigm for maintaining long-range consistency (Sahoo et al., 2024; Yu et al., 2025).

A key trend in dLLM evolution is the shift toward long-context generation (Liu et al., 2025a; He et al., 2025). This capability unlocks advanced applications such as repository-level code generation (Xie et al., 2025), novel generation, and massive-context information filling. However, despite their potential, deploying long-context dLLMs remains constrained by a prohibitive memory capacity barrier stemming from severe system inefficiencies.

Specifically, existing memory optimizations for LLMs prioritize the KV-cache (Kwon et al., 2023; Prabhu et al., 2025), the primary bottleneck in autoregressive generation; however, these techniques do not transfer to dLLMs. Our profiling reveals a fundamental shift: dLLMs are bottlenecked by *transient activations* recomputed at every step. While general-purpose reuse mechanisms address activation memory to some extent (Pisarchyk & Lee, 2020; Ansel et al., 2024), they lack the global visibility to adapt to dLLMs' *dynamic peaks*, which toggle between logits and FFNs. Consequently, applying existing methods results in significant fragmentation and redundancy, necessitating a system tailored to these distinct patterns.

To materialize this shift, we propose Mosaic, a memory-efficient inference system tailored for long-context dLLMs. Mosaic shifts from local, static management to a global, dynamic paradigm. We introduce a mask-only logits kernel that eliminates redundancy by computing logits solely for masked tokens. To handle dynamic bottlenecks, a lazy chunking optimizer employs an online search to split memory-intensive operators only when necessary, minimizing latency overhead. Underpinning these components is a global memory manager utilizing a graph registrar to capture the full computation lifecycle, enabling a unified virtual memory mapping that eliminates external fragmentation.

Our contributions are summarized as follows:

- We provide the first comprehensive characterization of dLLM memory usage, identifying the bottleneck shift to transient activations and the phenomenon of dynamic memory peaks.
- We propose Mosaic, a holistic system that integrates mask-only computation, virtual memory management, and a lazy chunking strategy driven by online heuristic search to adaptively identify the minimal configuration for efficient long-context inference.
- Extensive evaluations demonstrate that Mosaic eliminates external fragmentation and achieves an average $2.71 \times$ reduction in the memory peak-to-average ratio, extending the maximum inference sequence length supportable on identical hardware by $15.89\text{-}32.98 \times$. Notably, this comes without compromising accuracy and speed, and in fact reduces latency by 4.12%-23.26%.

2. Preliminaries

This section provides background on the inference paradigms of large language models (LLMs) and the memory management techniques used during inference. We focus on the distinctions between autoregressive (AR) and diffusion-based LLMs (dLLMs), as well as the memory characteristics that motivate our optimization.

2.1. LLM Inference Paradigms: From Autoregression to Diffusion

LLM inference converts an input prompt into an output text sequence. The dominant generation strategy has long been the autoregressive (AR) paradigm (Yang et al., 2025; Dubey et al., 2024), whereas recent diffusion-based LLMs (dLLMs), such as LLaDA (Nie et al., 2025) and Dream (Ye et al., 2025), introduce a fundamentally different inference workflow. Although both are typically implemented using the Transformer architecture (Vaswani et al., 2017), their inference pipelines have different computation patterns and memory behaviors as follows.

Autoregression. In AR models, inference proceeds sequentially. At each iteration, the model produces one new token, appends it to the current sequence, and feeds the extended sequence into the next iteration. This iterative process continues until the model emits an end-of-sequence (EOS) token or reaches the maximum generation length. Because each iteration depends on all previously generated tokens, the sequence length monotonically increases.

Diffusion. dLLMs use a non-autoregressive, iterative refinement process that generates *all* output tokens jointly. Given a prompt, a target output length L , and a specified number of inference steps N , the model begins with a fully masked sequence of length L . Over N iterative steps, the model gradually replaces masked tokens with sampled tokens.

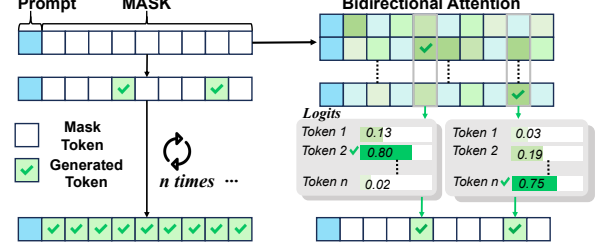


Figure 1. dLLM inference pipeline.

As illustrated in Figure 1, each diffusion step contains two stages: (1) Forward pass, where the model takes the prompt and the partially masked sequence as input and performs a single bidirectional forward pass, producing logits for all masked tokens simultaneously. (2) Sampling, where tokens are sampled from the logits and used to replace a selected subset of the [MASK] positions. Across iterations, the sequence progressively transitions from fully masked to fully specified.

Implications for Memory. Both AR and diffusion paradigms create substantial intermediate tensors (e.g., activations and KV-Cache), which scale with the context length and often exceed the memory footprint of model parameters. These tensors dominate inference memory usage and motivate the need for efficient memory management strategies.

2.2. LLM Memory Management Methods

LLM inference involves two types of memory-intensive data: (1) short-lived activations produced within a single forward pass, and (2) long-lived persistent caches such as the KV-cache in AR decoding. We summarize techniques for managing both as follows.

Managing Transient Activations via Memory Reuse. Intermediate activations have extremely short lifetimes: they are produced and consumed within the boundaries of a single forward pass. A standard approach to minimize memory consumption is graph-based memory planning, which analyzes the computation graph as a directed acyclic graph (DAG), where nodes are operations and edges are the activations flowing between them.

Through liveness analysis, the planner determines each activation's creation and last use. Activations whose lifetimes do not overlap can safely reuse the same memory buffer. This reuse reduces peak activation memory and has become the backbone of memory optimization in modern inference engines (Ansel et al., 2024; Pisarchyk & Lee, 2020; Lamprou et al., 2023).

Managing KV-Cache via Paging. In AR inference, causal attention ensures that keys and values for previously generated tokens remain unchanged across iterations. These

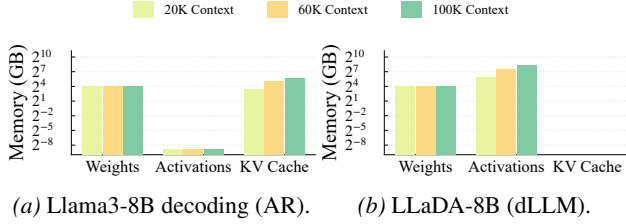


Figure 2. Memory breakdown of both LLMs.

tensors are therefore cached, forming the KV-cache, a persistent state whose lifetime spans the entire inference session (Li et al., 2024). Inference is typically divided into two phases: (1) Prefill, which computes the initial KV-cache from the prompt, and (2) Decode, which iteratively generates tokens while reading and extending the KV-cache.

Because KV-cache size grows linearly with sequence length, efficient storage is crucial. Page-based methods such as PagedAttention (Kwon et al., 2023) manage KV tensors in fixed-size blocks, reducing fragmentation and enabling flexible allocation and eviction policies. This strategy significantly lowers memory overhead and supports long-context AR generation.

3. Observations

As discussed in §2.1, efficient memory management is critical for enabling long-context inference. However, we find that conventional memory management techniques as described in §2.2, which is largely designed for autoregressive LLMs, do not directly transfer to diffusion-based LLMs (dLLMs). Through detailed profiling, we identify four observations that reveal fundamental mismatches between existing approaches and the memory characteristics of dLLM inference.

Observation #1: The Memory Bottleneck Shifts from KV-Cache to Transient Activations. We first analyze the memory breakdown of autoregressive and diffusion-based LLMs under increasing context lengths. Although intermediate tensors eventually exceed model weights in both paradigms, their composition differs substantially.

Figure 2a shows that during AR decoding, transient activations are computed only for the newly generated token at each step, while previously computed activations remain unchanged. In contrast, the KV-cache grows monotonically with sequence length and becomes the dominant memory consumer.

By comparison, dLLMs employ bidirectional attention, which causes key and value tensors to change at every diffusion step. As a result, caching is ineffective and each step must recompute transient activations for all tokens. Consequently, transient activations dominate memory usage, as

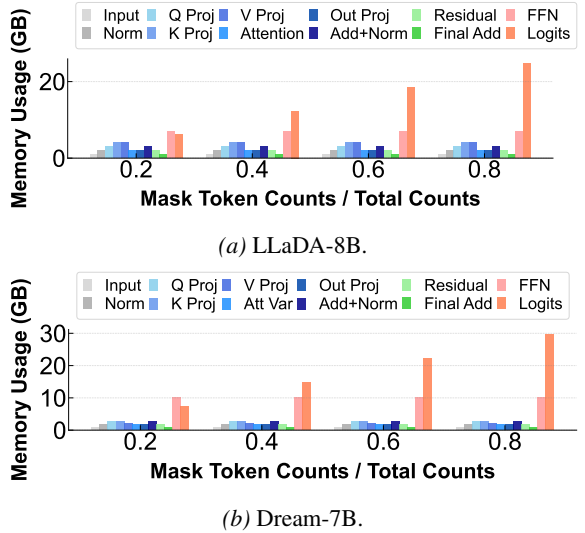


Figure 3. Dynamic memory bottleneck shift across varying mask ratios (r_m) at 128k context length. The memory peak **toggles** between Logits (at high r_m) and FFN (at low r_m).

shown in Figure 2b. This fundamental shift implies that memory management for dLLMs should move from a *KV-cache-centric* design toward a *transient-activation-centric* paradigm.

Observation #2: Logits Computation Wastes Memory on Unmasked Tokens. Given the dominance of transient activations in dLLMs, we observe that existing inference systems still compute logits for all tokens at each diffusion step because they overlook memory optimizations specific to dLLMs, even though only masked tokens are sampled (Nie et al., 2025; Ye et al., 2025; Ma et al., 2025). This eager computation incurs substantial and unnecessary memory overhead from non-masked logits.

Analogous to how the KV-cache eliminates redundant recomputation in AR models, an intuitive optimization is to compute logits only for masked tokens, which we call Mask-Only Logits. However, implementing this optimization is non-trivial: logits computation typically requires memory-contiguous inputs (Gale et al., 2020), while masked tokens are often scattered across the sequence. This tension complicates efficient realization of mask-only computation.

Observation #3: dLLM Inference Exhibits Dynamic Memory Peaks. Even with Mask-Only Logits, dLLM inference remains constrained by two major transient memory peaks: logits and FFN activations. As shown in Figure 3, the dominant peak varies dynamically with the mask ratio r_m , defined as the fraction of masked tokens. At low r_m , FFN activations dominate, whereas at high r_m , logits dominate. This behavior is consistent across models such as LLaDA-8B and Dream-7B.

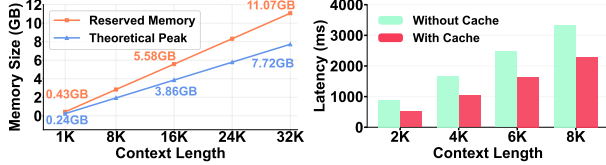


Figure 4. Reserved memory vs. Figure 5. Latency w/ and w/o theoretical peak.

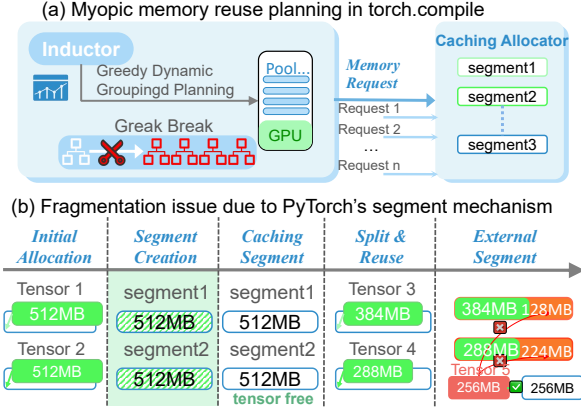


Figure 6. (a) Myopic planning. (b) Fragment issue.

This dynamic behavior arises from two factors: (1) Large feature dimensions, where both FFN intermediate sizes and vocabulary sizes are orders of magnitude larger than the hidden dimension, creating pronounced memory spikes; (2) Computation asymmetry, where FFNs operate over the full sequence, whereas logits are computed only for masked tokens. This asymmetry causes the relative memory footprint of logits and FFNs to vary with r_m , thereby leading to a dynamic shift in the memory peak. Together, these effects force systems to provision memory for the *worst-case* peak during generation, significantly limiting achievable context length.

Observation #4: Myopic Memory Planning Causes Severe Fragmentation. Unlike highly specialized AR inference engines, current dLLM frameworks typically rely on `torch.compile` together with a generic memory allocator (Paszke et al., 2019). We find that this combination introduces substantial memory overhead. Figure 4 shows that at a 32k context length, reserved memory exceeds the theoretical peak by 43.19%.

The root cause is myopic memory planning induced by graph partitioning. As illustrated in Figure 6(a), `torch.compile` frequently partitions execution into isolated subgraphs due to greedy grouping and fragile dynamic graph capture. Each subgraph independently requests contiguous memory regions, preventing global reuse across the full execution.

This fragmentation propagates to the physical allocator. To

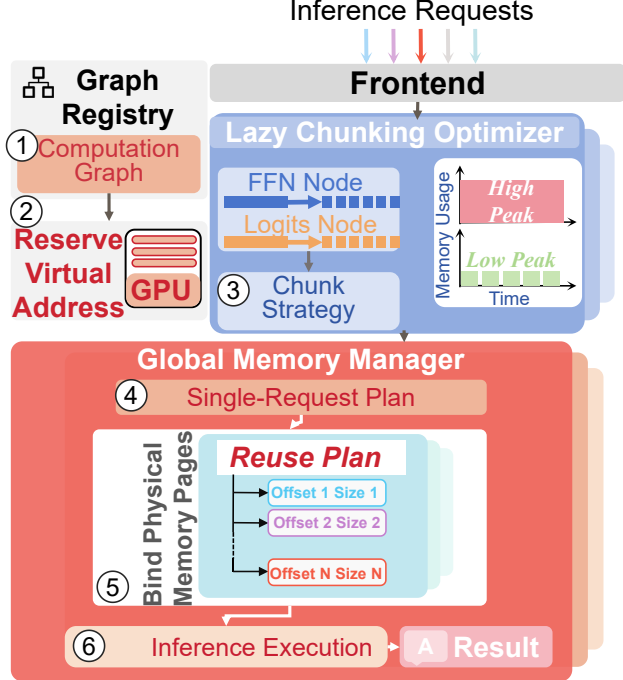


Figure 7. Mosaic's overview.

amortize allocation latency, which increases by 46%–72% without caching as in Figure 5, the allocator caches memory segments. However, independent allocation requests inevitably leave behind scattered free segments as in Figure 6(b). Because these fragments cannot be merged to satisfy large tensor allocations, the allocator repeatedly allocates new segments, resulting in external fragmentation and inflated reserved memory.

4. Design of Mosaic

4.1. Overview

We propose Mosaic, a system designed to enable long-context inference for diffusion-based LLMs. Mosaic consists of four tightly integrated components: (1) Mask-only logits kernel, which efficiently computes logits only for masked tokens without auxiliary memory allocation. (2) Graph registrar, which explicitly defines a parameterized computation graph to enable whole-graph visibility for chunk-wise execution and memory reuse planning. (3) Lazy chunking optimizer, which adaptively chunks memory-intensive operators (*i.e.*, FFN and logits) to reduce peak memory usage while minimizing latency overhead. (4) Global memory manager, which maps tensors into a virtually contiguous workspace to eliminate fragmentation.

As illustrated in Figure 7, Mosaic operates in two phases. In the offline phase, the graph registrar constructs a parameterized graph template using symbolic primitives once per

model ①. In the online phase, the global memory manager reserves a contiguous virtual address space ②. Upon receiving an inference request, the lazy chunking optimizer determines an appropriate chunking configuration via a bottleneck-driven search ③. The memory manager then generates a global reuse plan ④, binds physical pages to the virtual workspace according to the planned peak memory ⑤, and executes inference ⑥.

We begin by introducing the mask-only logits kernel, which forms the computational foundation of Mosaic. We then describe the graph registrar, lazy chunking optimizer, and global memory manager in sequence.

4.2. Mask-only Logits Kernel

To materialize the Mask-Only strategy (Observation #2), Mosaic must overcome a challenge: Logits computation is a GEMM (General Matrix Multiply) operation requiring memory-contiguous input, but masked tokens are scattered in memory. A naive approach involves allocating a new contiguous buffer and gathering the masked hidden states before inputting them to the GEMM, but this causes memory overhead for the intermediate buffer.

Mosaic introduces a gather-GEMM fused kernel to directly process scattered inputs. The kernel accepts all token hidden states and mask indices (identifying masked tokens), partitions computation into tiles handled by parallel GPU compute units. Each unit processes multiple tiles sequentially: it uses mask indices to perform indirect addressing via pointer arithmetic, fetches scattered data into on-chip memory, performs matrix multiplication, and accumulates partial results. Tiles are discarded after each iteration, eliminating intermediate buffers in GPU global memory.

This tile-based approach pipelines addressing and computation to overlap execution, achieving high hardware efficiency in a single kernel launch. It achieves 4.12%-23.26% reduction in end-to-end latency by skipping non-masked token computations, as demonstrated in our evaluation (§5.2).

4.3. Graph Registrar

The lazy chunking optimizer and the global memory manager in Mosaic fundamentally rely on a complete computation graph for chunk-wise analysis and memory reuse planning. However, existing compiler-level dynamic capture is often fragile, where incompatible code triggers graph breaks that split the computation into separate sub-graphs. Therefore, we introduce the graph registrar to explicitly define a parameterized graph template as the foundation for these components.

As shown in Figure 8, we developed a lightweight graph registration system that provides a set of symbolic primitives for graph definition. Instead of relying on unstable dynamic

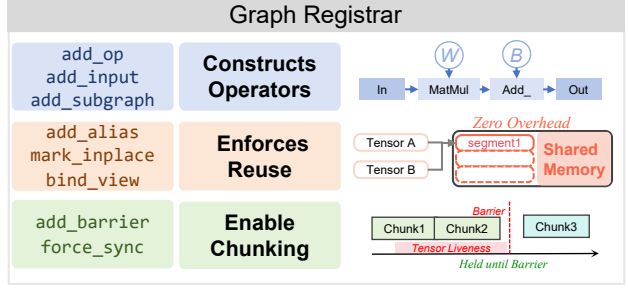


Figure 8. Mosaic’s graph registrar.

capture, we utilize these primitives (e.g., `add_op()`) to define a parameterized graph template. This template captures the model’s topological structure and memory dependencies while leaving input-dependent dimensions (e.g., sequence lengths) as symbolic variables to be instantiated at runtime. This guarantees an unbroken view of the entire model structure. Furthermore, the system includes constraint primitives such as `add_alias()` to enforce memory aliasing (*i.e.*, binding a module’s output address to the next module’s input to ensure seamless connection).

Finally, to support the lazy chunking optimizer, the registrar incorporates chunk-wise primitives. It allows defining operators with symbolic chunk sizes and introduces control primitives such as `add_barrier()`. These barriers explicitly extend the lifespan of input tensors to cover the entire chunking loop, preventing the memory manager from reclaiming them before all chunks are processed.

4.4. Lazy Chunking Optimizer

As analyzed in §3, the memory bottleneck shifts dynamically between logits and FFN depending on the mask ratio (r_m). A naive solution is to split these operations along the sequence dimension. However, this introduces two critical challenges: 1) Latency overhead. Decomposing a single large kernel into multiple small launches adds extra execution overhead. 2) Misaligned configuration. Since the bottleneck moves, a static policy might chunk the wrong component (*e.g.*, chunking FFN when logits is the peak), which increases latency without reducing peak memory. To address these challenges, Mosaic proceeds in three stages. First, it analyzes the latency impact to identify the opportunity to chunk at long context. Guided by this, it introduces a lazy chunking strategy to minimize latency overhead. Crucially, to materialize this strategy under dynamic bottlenecks, we devise an online bottleneck-driven search to accurately determine the minimal sufficient chunk configuration.

Opportunity to chunk at long context. As shown in Figure 9, we measured the latency impact on FFN and logits computations across different context lengths and chunk

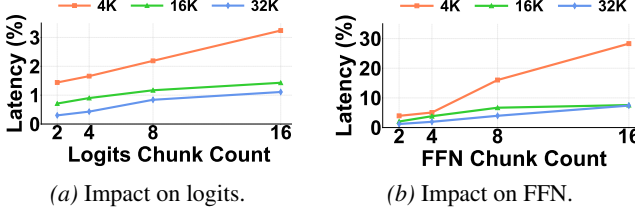


Figure 9. Latency analysis of chunked execution across different context lengths and chunk counts.

counts. We observe that the relative latency increase gets smaller as the context length increases and the chunk count decreases. For instance, at 32K context with 4 chunks, the latency increase is less than 0.5% for Logits and 2% for FFN. This is because long contexts saturate the GPU, causing latency to grow linearly. As a result, the total time of chunked execution is nearly the same as executing it as a whole, making the overhead negligible.

Lazy chunking strategy. Based on this observation, we introduce a lazy chunking strategy. To minimize overhead, we disable chunking by default and activate it only when the physical memory is insufficient for the target context length. Since memory shortages primarily occur at long context, this ensures that chunking is triggered precisely in the low-overhead regime.

When activated, this strategy employs parameters K_{logits} and K_{FFN} to control chunk counts for the logits and FFN operations, respectively. To ensure efficiency, we must identify the minimal configuration that exactly supports the target context. However, determining this configuration is non-trivial because the memory bottleneck shifts dynamically with the mask ratio (r_m). Consequently, we employ an online bottleneck-driven search to solve this configuration dilemma.

Online bottleneck-driven search. To instantiate the lazy chunking strategy, we need to find a feasible chunk setting. A naive solution is to brute-force search all chunk combinations. However, this incurs prohibitive runtime overhead. Crucially, we observe that due to memory reuse, the total footprint is dictated by the single highest peak and reducing non-dominant components yields zero gain. Leveraging this insight, we prune the search space and employ a bottleneck-driven heuristic search. To guarantee consistency with runtime execution, we instantiate the registrar’s graph template with candidate chunk parameters and simulate the exact buffer size by invoking the global memory manager’s planner.

The search accepts the number of masks and total tokens as runtime inputs. It targets the current bottleneck, increments K_{logits} or K_{FFN} by 1, and re-evaluates the memory usage to identify the new peak. The search repeats this process and

halts immediately when the peak fits within the available memory or reaches the peak of non-chunkable components (signaling insufficient capacity). This heuristic identifies the minimal sufficient chunk settings with negligible overhead, and the derived K_{logits} and K_{FFN} are immediately applied to the runtime execution.

4.5. Global Memory Manager

To eliminate fragmentation described in §3, we identify the root cause as the fact that issuing multiple separate requests implicitly delegates the tensor placement decision (i.e., assigning each logical memory request to a specific physical segment) to the underlying allocator. Lacking a global view, this delegation inevitably leads to fragmentation.

Therefore, we can eliminate this issue by generating a single global memory request to explicitly bypass the tensor placement decision within the physical allocator. To enable this single request, we treat the workspace as a unified address space and pre-calculate a reuse plan specifying the exact offset and size for every tensor to direct the runtime execution.

Accordingly, Mosaic implements this mechanism via two core components: 1) a single-request planner, which performs whole-graph analysis to derive the plan; and 2) a VMM-based allocator, which efficiently maps physical pages to the planned addresses. Next, we describe the two components in detail.

Single-request planner. Constructing a unified reuse plan requires observing the complete lifecycles of all transient tensors. We achieve this by deriving the computation graph from the registrar’s templates, integrated with the lazy chunking strategy. This visibility enables us to perform reuse planning, determining all tensors’ offsets.

While finding the optimal offsets is an NP-hard problem solvable via integer linear programming (ILP) (Steiner et al., 2023), our evaluation (§5.3) indicates that ILP solvers incur prohibitive latency. Therefore, we adopt a first-fit heuristic, which reduces planning time to merely 0.1%-4.3% of the ILP while achieving the same supportable context length. This confirms first-fit as an ideal choice for memory planning.

VMM-based allocator. Since the planner maps all tensors into a unified address space, the workspace buffer must be contiguous to support it. However, a naive static pre-allocation would lead to substantial memory waste (under-utilization) when handling short sequences. To resolve this conflict between contiguity and efficiency, Mosaic leverages a virtual memory management (VMM) based allocator.

Specifically, during initialization, we only reserve a large range of contiguous virtual addresses, which does not oc-

copy any physical memory. At runtime, once the planned peak memory is known, we dynamically bind physical pages to this virtual range using low-level page mapping APIs. This ensures that the execution sees a contiguous buffer while the actual physical consumption is strictly limited to the planned peak memory, eliminating overhead from idle pre-allocations.

With the physical memory mapped, Mosaic executes inference following the reuse plan. Since standard PyTorch operators typically allocate new memory for outputs, we replace them with custom in-place variants that write results directly to target offsets. Importantly, certain in-place optimizations inherently reduce memory demand, such as replacing Dream’s unique logits shift and concatenation with a memory-saving, token-level alternative.

5. Evaluation

5.1. Experimental Setup

Implementation. We implemented Mosaic based on vLLM to use its robust serving infrastructure. To enable dLLM inference, we integrated the official PyTorch model code and bypassed vLLM’s standard KV-Cache components, replacing them with dLLM-specific inference logic. Additionally, the system supports variable-length inference to eliminate padding and implements iteration-level scheduling for efficient execution control.

Hardware Setup. We evaluated Mosaic on an NVIDIA GeForce RTX 3090 with 24GB VRAM and an NVIDIA A100 with 40GB VRAM.

Models and Workloads. We evaluate three mainstream dLLMs: LLaDA-8B, Dream-7B, and LLaDA-MoE. Since Mosaic supports context lengths that significantly exceed the models’ native training limits, we utilize dummy input. This enables us to evaluate Mosaic’s true maximum context length and performance.

Baselines. We compare Mosaic against three key baselines to ensure a fair comparison and validate our optimization contributions: (1) Native: The unmodified official PyTorch code. This measures the raw performance without any serving infrastructure; (2) Mosaic-Torch: The PyTorch model code ported onto the vLLM framework (enabling varlen), without memory optimizations, which proves our framework migration is lossless; (3) Mosaic-Compile: This baseline integrates `torch.compile` into the Mosaic-Torch.

Key Metrics. We evaluate Mosaic and baselines based on two metrics: 1) Per-step latency, which measures the time for a single diffusion step; 2) Maximum context length (L_{\max}), quantifies the largest context size supportable before an Out-of-Memory (OOM) error.

5.2. End-to-end Evaluation

For a comprehensive evaluation, we selected requests with varying ratios of prompt length to output length (denoted as r_p , which corresponds to the initial r_m) for each model. Figure 10 illustrates the latency and maximum supportable context length of Mosaic and the baselines. Mosaic consistently outperforms all alternatives in L_{\max} . Its L_{\max} is 32.98, 26.74, and 15.89 times that of Native, Mosaic-Torch, and Mosaic-Compile, respectively. Furthermore, Mosaic achieves this without compromising latency; in fact, it shows an average 4.12%–23.26% reduction compared to Mosaic-Torch and Mosaic-Compile, as shown in Figure 11. To understand the performance difference, we conjecture that Mosaic’s advantage arises from three key factors, outlined as follows.

First, existing systems fail to handle memory peaks, thereby bounding the context capacity. In contrast, Mosaic employs lazy chunking to mitigate this issue. It addresses memory spikes by chunking peak activations when memory is insufficient for longer contexts. As shown in Figure 12, we utilize the memory’s peak-to-average ratio to quantify the fluctuation of activation memory usage. Mosaic exhibits a significantly lower ratio when chunking is enabled (the ratio is lower even before chunking activates because the mask-only kernel reduces logits memory), achieving an average $2.71 \times$ reduction. This effectively resolves spikes, which directly translates to a higher L_{\max} .

Secondly, existing systems rely on myopic memory planning, leading to external fragmentation and inflated reserved memory compared to the theoretical peak (21.78%–78.33% inflation rate in Figure 13). In contrast, Mosaic employs a global manager to eliminate external fragmentation and optimize operators for in-place execution (*e.g.*, replacing Dream’s unique logits shift with a memory-saving, token-level alternative), collectively enabling a larger L_{\max} .

Thirdly, Mosaic incurs no compromise on latency, achieving a 4.12%–23.26% reduction. This improvement is attributed to mask-only logits kernel eliminating redundant computations and graph registration system bypassing the dynamic graph capture overhead inherent in `torch.compile`.

5.3. Ablation Study

In this section, we disable each of Mosaic’s novel features to demonstrate its contribution to extending L_{\max} without compromising latency. Due to space limitations, we only present results for $r_p = 0.5$, as performance on other r_p is similar.

Breakdown of L_{\max} improvements. To quantify the contribution of each component to L_{\max} , we performed a cumulative breakdown of the performance gains. Starting with the Mosaic-Torch baseline, we incrementally integrated the

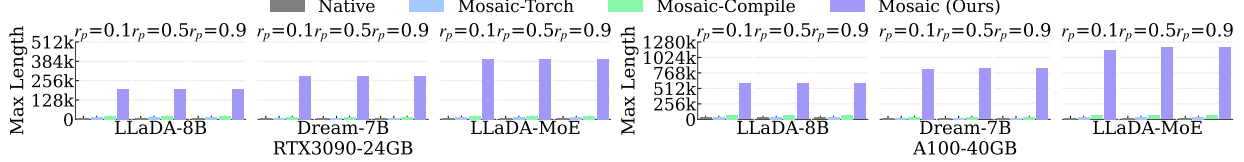


Figure 10. End-to-end performance evaluation. Comparison of latency and L_{\max} for Mosaic and baselines across varying prompt-to-output ratios (r_p).

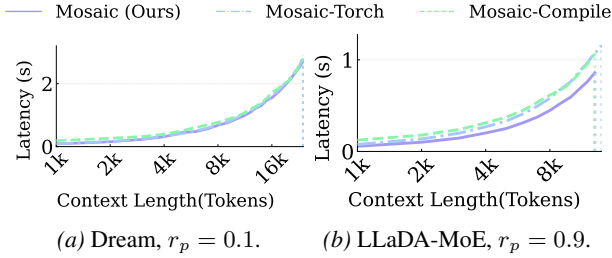


Figure 11. Latency reduction extremes: (a) minimum with Dream at $r_p = 0.1$ (avg. 4.12%) and (b) maximum with LLaDA-MoE at $r_p = 0.9$ (avg. 23.26%).

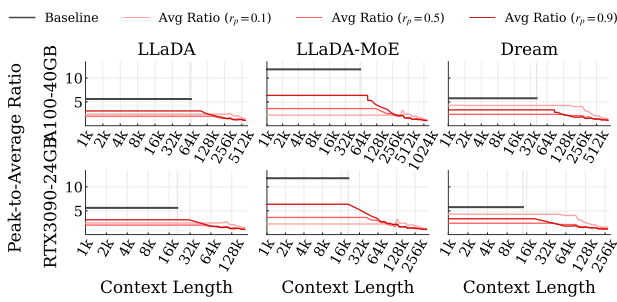


Figure 12. Comparison of activation memory peak-to-average ratio (PAR) across context lengths.

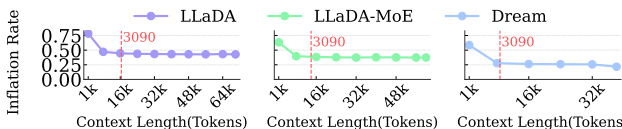


Figure 13. Inflation rates of baselines.

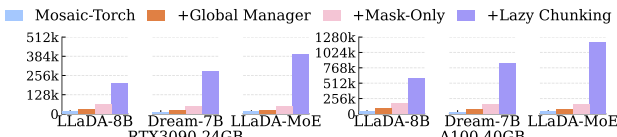


Figure 14. Impact of the global memory manager, mask-only kernel, and lazy chunking on L_{\max} .

global memory manager, mask-only kernel, and lazy chunking optimizer.

As shown in Figure 14, the global manager extends L_{\max} by 79.0%–197.1% through global memory reuse coupled

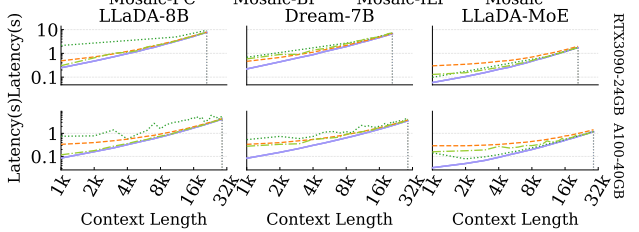


Figure 15. Ablation study of inference latency comparing planning, search, and chunking strategies.

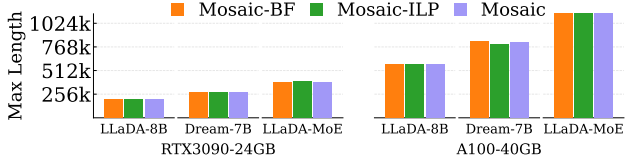


Figure 16. Comparison of L_{\max} using different search strategies (Brute-force vs. Bottleneck-driven) and planning algorithms (ILP vs. First-fit).

with optimized in-place operators (e.g., replacing Dream’s unique logits shift and concatenation with a memory-saving, token-level alternative). The mask-only kernel provides an additional 88.9%–114.3% gain by discarding the logits memory of unmasked tokens, while lazy chunking further boosts L_{\max} by 221.3%–673.3% by mitigating memory spikes.

Impact of chunking strategy. Mosaic employs a lazy chunking strategy to mitigate the latency overhead induced by chunking operations. To evaluate its effectiveness, we compare Mosaic against Mosaic-FC, a baseline that statically applies the L_{\max} chunking configuration across all context lengths.

As shown in Figure 15, Mosaic achieves a 5.5%–21.5% latency reduction within the 32k context range. This reduction is particularly pronounced at shorter context lengths, where the relative overhead of chunking is higher. By dynamically disabling chunking for short contexts, Mosaic effectively eliminates this unnecessary overhead.

Efficiency of bottleneck-driven search. Mosaic employs a bottleneck-driven heuristic to search for chunking configurations online. To evaluate its efficiency, we compare Mosaic

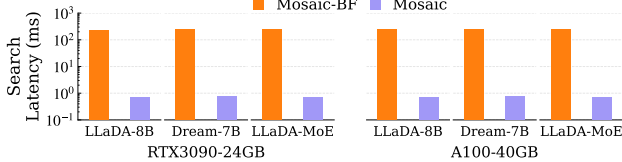


Figure 17. Comparison of search latency.

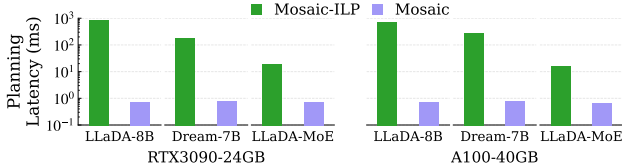


Figure 18. Comparison of planning latency.

against Mosaic-BF, a variant utilizing brute-force search.

While matching the L_{\max} of Mosaic-BF (Figure 16), Mosaic incurs only 0.28%-0.32% of the search latency (Figure 17), reducing overall short-context latency by 22.3%-70.7% (Figure 15). This confirms that our heuristic finds optimal configurations with minimal search latency, and the advantage diminishes in long contexts dominated by model computation.

Efficiency of first-fit planning. Mosaic employs a first-fit strategy to determine tensor offsets. We compare it against Mosaic-ILP, a baseline utilizing integer linear programming (ILP) for theoretically optimal planning.

As shown in Figure 16, both strategies achieve identical L_{\max} . This is because lazy chunking reduces peak memory to that of non-chunkable components as context grows. Consequently, the planning task simplifies to packing tensors within this fixed capacity, a task where the first-fit heuristic performs as effectively as ILP. However, first-fit incurs only 0.1%-4.3% of the planning latency (Figure 18), reducing overall latency by 7.1%-36.7% due to its significantly lower algorithmic complexity (Figure 15).

6. Related Work

Diffusion Language Models and Optimization. Text diffusion has evolved from continuous approximations (Li et al., 2022; Gong et al., 2022) to discrete token-space formulations (Austin et al., 2021; Han et al., 2023), culminating in Transformer-based dLLMs (Nie et al., 2025; Ye et al., 2025) that leverage bidirectional attention for superior global planning. To accelerate inference, one line of work introduces KV-caching (Wu et al., 2025); however, this re-introduces the persistent memory-intensive KV bottleneck and may compromise generation quality (Wu et al., 2025; Liu et al., 2025b; Hu et al., 2025b). In contrast, we target the standard bidirectional dLLMs to ensure strict global consistency.

Activation Memory Reuse. Mainstream frameworks optimize memory via liveness analysis (Pisarchyk & Lee, 2020; Ansel et al., 2024). However, fragile *dynamic capture* often triggers “graph breaks” (Ansel et al., 2024) that produce isolated sub-graphs, resulting in suboptimal reuse.

Persistent State Memory Optimization. Systems like vLLM (Kwon et al., 2023) and vAttention (Prabhu et al., 2025) optimize AR inference by managing the persistent KV-cache via paging or virtual memory. Additionally, KV-Cache offloading is commonly utilized to alleviate the memory pressure (Hu et al., 2025a), while prefix-aware attention is employed to accelerate inference by aggregating KV states (Yi et al., 2025). However, these are ill-suited for bidirectional dLLMs.

7. Conclusion

In this paper, we identified the fundamental mismatch between conventional memory management and the unique requirements of diffusion-based LLMs, specifically the shift from KV-cache to transient activations and dynamic memory peaks. To bridge this gap, we proposed Mosaic, a system that harmonizes mask-only computation, global graph planning, and adaptive lazy chunking. Mosaic effectively eliminates redundancy and fragmentation, enabling 15.89-32.98 \times longer context length with reduced peak memory and comparable latency. Our work paves the way for scalable dLLM inference, making long-context applications more accessible and efficient.

References

- Ansel, J., Yang, E., He, H., Gimelshein, N., Jain, A., Voznesensky, M., Bao, B., Bell, P., Berard, D., Burovski, E., et al. Pytorch 2: Faster machine learning through dynamic python bytecode transformation and graph compilation. In *Proceedings of the 29th ACM International Conference on Architectural Support for Programming Languages and Operating Systems, Volume 2*, pp. 929–947, 2024.
- Austin, J., Johnson, D. D., Ho, J., Tarlow, D., and Van Den Berg, R. Structured denoising diffusion models in discrete state-spaces. *Advances in neural information processing systems*, 34:17981–17993, 2021.
- Dubey, A., Jauhri, A., Pandey, A., Kadian, A., Al-Dahle, A., Letman, A., Mathur, A., Schelten, A., Yang, A., Fan, A., et al. The llama 3 herd of models. *arXiv preprint arXiv:2407.21783*, 2024.
- Gale, T., Zaharia, M., Young, C., and Elsen, E. Sparse gpu kernels for deep learning. In *SC20: International Conference for High Performance Computing, Networking, Storage and Analysis*, pp. 1–14. IEEE, 2020.

Gong, S., Li, M., Feng, J., Wu, Z., and Kong, L. Diffuseq: Sequence to sequence text generation with diffusion models. *arXiv preprint arXiv:2210.08933*, 2022.

Han, X., Kumar, S., and Tsvetkov, Y. Ssd-lm: Semi-autoregressive simplex-based diffusion language model for text generation and modular control. In *Proceedings of the 61st Annual Meeting of the Association for Computational Linguistics (Volume 1: Long Papers)*, pp. 11575–11596, 2023.

He, G., Nie, S., Zhu, F., Zhao, Y., Bai, T., Yan, R., Fu, J., Li, C., and Yuan, B. Ultrallada: Scaling the context length to 128k for diffusion large language models. *arXiv preprint arXiv:2510.10481*, 2025.

Hu, Y., Liu, X., Yang, G., Li, L., Zeng, K., Zhao, Z., Chen, S., Zhao, L., Li, W., and Li, K. Tightllm: Maximizing throughput for llm inference via adaptive offloading policy. *IEEE Transactions on Computers*, 2025a.

Hu, Z., Meng, J., Akhauri, Y., Abdelfattah, M. S., Seo, J.-s., Zhang, Z., and Gupta, U. Accelerating diffusion language model inference via efficient kv caching and guided diffusion. *arXiv preprint arXiv:2505.21467*, 2025b.

Kwon, W., Li, Z., Zhuang, S., Sheng, Y., Zheng, L., Yu, C. H., Gonzalez, J., Zhang, H., and Stoica, I. Efficient memory management for large language model serving with pagedattention. In *Proceedings of the 29th symposium on operating systems principles*, pp. 611–626, 2023.

Lamprou, I., Zhang, Z., de Juan, J., Yang, H., Lai, Y., Filhol, E., and Bastoul, C. Safe optimized static memory allocation for parallel deep learning. *Proceedings of Machine Learning and Systems*, 5:305–324, 2023.

Li, H., Li, Y., Tian, A., Tang, T., Xu, Z., Chen, X., Hu, N., Dong, W., Li, Q., and Chen, L. A survey on large language model acceleration based on kv cache management. *arXiv preprint arXiv:2412.19442*, 2024.

Li, X., Thickstun, J., Gulrajani, I., Liang, P. S., and Hashimoto, T. B. Diffusion-lm improves controllable text generation. *Advances in neural information processing systems*, 35:4328–4343, 2022.

Liu, X., Song, Y., Liu, Z., Huang, Z., Guo, Q., He, Z., and Qiu, X. Longllada: Unlocking long context capabilities in diffusion llms. *arXiv preprint arXiv:2506.14429*, 2025a.

Liu, Z., Yang, Y., Zhang, Y., Chen, J., Zou, C., Wei, Q., Wang, S., and Zhang, L. dllm-cache: Accelerating diffusion large language models with adaptive caching. *arXiv preprint arXiv:2506.06295*, 2025b.

Ma, Y., Du, L., Wei, L., Chen, K., Xu, Q., Wang, K., Feng, G., Lu, G., Liu, L., Qi, X., et al. dinfer: An efficient inference framework for diffusion language models. *arXiv preprint arXiv:2510.08666*, 2025.

Minaee, S., Mikolov, T., Nikzad, N., Chenaghlu, M., Socher, R., Amatriain, X., and Gao, J. Large language models: A survey. *arXiv preprint arXiv:2402.06196*, 2024.

Nie, S., Zhu, F., You, Z., Zhang, X., Ou, J., Hu, J., Zhou, J., Lin, Y., Wen, J.-R., and Li, C. Large language diffusion models. *arXiv preprint arXiv:2502.09992*, 2025.

Paszke, A., Gross, S., Massa, F., Lerer, A., Bradbury, J., Chanan, G., Killeen, T., Lin, Z., Gimelshein, N., Antiga, L., et al. Pytorch: An imperative style, high-performance deep learning library. *Advances in neural information processing systems*, 32, 2019.

Pisarchyk, Y. and Lee, J. Efficient memory management for deep neural net inference. *arXiv preprint arXiv:2001.03288*, 2020.

Prabhu, R., Nayak, A., Mohan, J., Ramjee, R., and Panwar, A. vattention: Dynamic memory management for serving llms without pagedattention. In *Proceedings of the 30th ACM International Conference on Architectural Support for Programming Languages and Operating Systems, Volume 1*, pp. 1133–1150, 2025.

Sahoo, S., Arriola, M., Schiff, Y., Gokaslan, A., Marroquin, E., Chiu, J., Rush, A., and Kuleshov, V. Simple and effective masked diffusion language models. *Advances in Neural Information Processing Systems*, 37:130136–130184, 2024.

Steiner, B., Elhoushi, M., Kahn, J., and Hegarty, J. Model: memory optimizations for deep learning. In *International Conference on Machine Learning*, pp. 32618–32632. PMLR, 2023.

Vaswani, A., Shazeer, N., Parmar, N., Uszkoreit, J., Jones, L., Gomez, A. N., Kaiser, Ł., and Polosukhin, I. Attention is all you need. *Advances in neural information processing systems*, 30, 2017.

Wu, C., Zhang, H., Xue, S., Liu, Z., Diao, S., Zhu, L., Luo, P., Han, S., and Xie, E. Fast-dllm: Training-free acceleration of diffusion llm by enabling kv cache and parallel decoding. *arXiv preprint arXiv:2505.22618*, 2025.

Xie, Z., Ye, J., Zheng, L., Gao, J., Dong, J., Wu, Z., Zhao, X., Gong, S., Jiang, X., Li, Z., et al. Dream-coder 7b: An open diffusion language model for code. *arXiv preprint arXiv:2509.01142*, 2025.

Yang, A., Li, A., Yang, B., Zhang, B., Hui, B., Zheng, B., Yu, B., Gao, C., Huang, C., Lv, C., et al. Qwen3 technical report. *arXiv preprint arXiv:2505.09388*, 2025.

Ye, J., Xie, Z., Zheng, L., Gao, J., Wu, Z., Jiang, X., Li, Z., and Kong, L. Dream 7b: Diffusion large language models. *arXiv preprint arXiv:2508.15487*, 2025.

Yi, J., Zhao, Z., Hu, Y., Yan, K., Sun, W., Wang, H., Zhao, L., Zhang, Y., Li, W., and Li, K. Pat: Accelerating lilm decoding via prefix-aware attention with resource efficient multi-tile kernel. *arXiv preprint arXiv:2511.22333*, 2025.

Yu, R., Li, Q., and Wang, X. Discrete diffusion in large language and multimodal models: A survey. *arXiv preprint arXiv:2506.13759*, 2025.

Zhao, W. X., Zhou, K., Li, J., Tang, T., Wang, X., Hou, Y., Min, Y., Zhang, B., Zhang, J., Dong, Z., et al. A survey of large language models. *arXiv preprint arXiv:2303.18223*, 1(2), 2023.

Zhu, F., You, Z., Xing, Y., Huang, Z., Liu, L., Zhuang, Y., Lu, G., Wang, K., Wang, X., Wei, L., et al. Llada-moe: A sparse moe diffusion language model. *arXiv preprint arXiv:2509.24389*, 2025.